Polymer Chemistry

RSC Publishing

PAPER

One-pot controlled synthesis of double thermoresponsive *N*-vinylcaprolactam-based copolymers with tunable LCSTs†

Cite this: *Polym. Chem.*, 2013, **4**, 2575

Anthony Kermagoret,[a] Charles-André Fustin,[b] Maxime Bourguignon,[a] Christophe Detrembleur,[a] Christine Jérôme[a] and Antoine Debuigne*[a]

Received 25th January 2013
Accepted 15th February 2013

DOI: 10.1039/c3py00134b

www.rsc.org/polymers

N-Vinylcaprolactam (*N*VCL) was copolymerized statistically for the first time in a controlled manner with hydrophilic *N*-vinylamide or hydrophobic vinylester monomers in order to precisely tune up and down the lower critical solution temperature (LCST) of the resulting copolymers. The incorporation of these segments in complex architectures was also considered. Several narrowly distributed *N*VCL-based copolymers were prepared by cobalt-mediated radical polymerization (CMRP) using the bis-(acetylacetonato)cobalt(II) complex as a controlling agent and *N*-methyl-*N*-vinylacetamide (*N*MVA), *N*-vinylacetamide (*N*VA), vinyl acetate (VAc) or vinyl pivalate (VPi) as comonomers. P*N*VCL-containing block copolymers having two discrete LCSTs were also synthesized following a one-pot strategy based on the sequential CMRP of *N*VCL followed by the copolymerization of *N*MVA with the residual *N*VCL. Upon gradual heating of aqueous solutions of such double thermoresponsive copolymers, we noticed a transition from free chains to micelles before full dehydration and collapse of the block copolymers. These advances represent a significant step towards the development of a platform based on thermoresponsive P*N*VCL copolymers with a single phase separation or multistep assembly behaviors.

Introduction

The last ten years have seen the tremendous development of stimuli-responsive macromolecules[1–3] valuable in a wide range of applications in biomedicine, microelectronics and pharmaceutics.[4,5] In particular, thermoresponsive polymers, whose solvation state suddenly changes at a critical temperature, have been exploited for the design of "smart" materials including drug release systems, bio-sensors or scaffolds. Some of these (co)polymers are characterized by an upper critical solution temperature (UCST) and solubilize upon heating[6] while others exhibit a lower critical solution temperature (LCST) above which they become insoluble.[7] Poly(*N*-isopropylacrylamide),[8–11] poly(2-oxazoline),[12,13] and oligo(ethylene glycol)methacrylate-based (co)polymers[14–16] are currently the most studied thermoresponsive polymers. In addition, some multiple thermoresponsive block copolymers have attracted attention due to their complex multistep assembly behavior[17–25] and their potential in the development of reversible encapsulation and release systems.

Recently, there has been an increasing interest in the use of poly(*N*-vinylcaprolactam) (P*N*VCL) due to its biocompatibility[26–28] and because its heat-induced precipitation in water (LCST transition) occurs close to the physiological temperature.[29] In addition, variation of the dehydration temperature of P*N*VCL in water was reported by introduction of comonomers within the chain.[30,31] For example, the LCST of P*N*VCL was increased from 33 °C to 60 °C and 77 °C by statistical copolymerization with *N*-vinylformamide (*N*VF) (80 mol%)[30] and *N*-methyl-*N*-vinylacetamide (*N*MVA) (66 mol%),[31] respectively. In contrast, LCST as low as 5 °C was recorded for P(*N*VCL-*co*-VAc) copolymers having 66 mol% of VAc content.[31] Although these studies provide interesting trends on the thermal behavior of the P*N*VCL statistical copolymers in water, they suffer from significant limitations. Indeed, the above-mentioned copolymers were prepared by free radical polymerization (FRP), which does not ensure that all the copolymer chains have the same composition and does not allow any control of the molar mass of the copolymers, while these two parameters dramatically influence the LCST of the P*N*VCL containing copolymers.[32] Moreover, these thermo-sensitive copolymers prepared by FRP cannot be incorporated into complex architectures, like block copolymers, for the design of temperature triggered self-assembled systems.

[a]*Center for Education and Research on Macromolecules (CERM), Chemistry Department, University of Liège (ULg), Sart-Tilman, Allée de la Chimie 3, Bat. B6a, B-4000 Liège, Belgium. E-mail: adebuigne@ulg.ac.be; Tel: +32 43663565*

[b]*Institute of Condensed Matter and Nanosciences (IMCN), Bio- and Soft Matter division (BSMA), Université catholique de Louvain, Place Pasteur 1, 1348 Louvain-la-Neuve, Belgium*

† Electronic supplementary information (ESI) available: Additional structural characterizations and thermal response studies of the copolymers were carried out by nuclear magnetic resonance, dynamic light scattering, turbidimetry and electronic microscopy. See DOI: 10.1039/c3py00134b

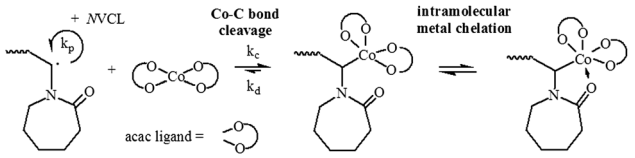

Scheme 1 General mechanism for the cobalt-mediated radical polymerization of *N*-vinylcaprolactam.

N-Vinylcaprolactam (*N*VCL) is a non-conjugated vinyl monomer and the absence of a stabilizing group for the propagating radical renders the control of its polymerization challenging. Only a few controlled radical polymerization (CRP) techniques can properly mediate the radical polymerization of *N*VCL including macromolecular design *via* interchange of xanthate (MADIX)[32,33] and more recently cobalt-mediated radical polymerization (CMRP) (Scheme 1).[34,35] The latter is an organometallic-mediated radical polymerization technique (OMRP)[36–38] based on the temporary deactivation of the growing radical polymer chains by a cobalt(II) complex.[39] For example, bis-(acetylacetonato)cobalt(II) ($Co(acac)_2$) has proven its ability to control efficiently the polymerization of the non-conjugated *N*-vinyl amides[34,35] and vinyl esters[40] including *N*VCL,[34,35] *N*MVA,[34] *N*-vinylpyrrolidone (*N*VP),[41,42] vinyl acetate (VAc),[40,43] vinyl pivalate (VPi)[44] and vinyl stearate.[45] Recent studies evidenced the preponderance of an intramolecular metal chelation phenomenon in the mechanism of the CMRP of these monomers (Scheme 1).[34,43] Indeed, the amide or ester moiety of the last monomer unit of the chain chelates the cobalt which reinforces the cobalt–polymer bond and stabilizes the dormant species.[34,43] Several polymer architectures have been prepared by CMRP[36,39] in the last few years including the design of thermoresponsive PVAc-*block*-P*N*VCL and poly(vinyl alcohol)-*block*-P*N*VCL block copolymers.[35]

In this contribution, we report the first controlled statistical radical copolymerization of *N*VCL with hydrophilic *N*-vinylamides and hydrophobic vinyl esters in order to precisely tune up and down the LCST of P*N*VCL over a wide range of temperatures and to possibly incorporate these segments into more complex architectures. Several narrowly distributed statistical copolymers with different compositions were prepared by CMRP and the phase transition temperatures of the corresponding aqueous solutions were measured by turbidimetry. Based on these advances, we developed a one-pot straightforward synthetic strategy for novel *N*VCL-based block copolymers displaying two discrete LCSTs; a homo-P*N*VCL block is connected to a statistical P(*N*VCL-*stat*-*N*MVA) copolymer characterized by a higher LCST. The complex thermal behavior of such double thermoresponsive copolymers in water was assessed by turbidimetry, dynamic light scattering (DLS), transmission electronic microscopy (TEM) and nuclear magnetic resonance (NMR) analyses. Upon gradual heating of the copolymer aqueous solutions, we noticed a transition from free chains to micelles before full dehydration and collapse of the block copolymer. The reversibility of the thermal-induced phase transitions was also investigated.

Experimental section

Materials

Vinyl acetate (VAc, >99%, Aldrich), *N*-methyl-*N*-vinylacetamide (*N*MVA, 98%, Aldrich) and vinyl pivalate (VPi, 99%, Aldrich) were dried over calcium hydride, degassed by several freeze–thawing cycles before distillation under reduced pressure and stored under argon. *N*-Vinylcaprolactam (*N*VCL, 98%, Aldrich) and *N*-vinylacetamide (*N*VA, 98%, TCI) were used as received. Bis-(acetylacetonato)cobalt(II) ($Co(acac)_2$) (>98%, Acros) was stored under argon and used as received. 2,2,6,6-Tetramethylpiperidine-1-oxyl (TEMPO, 98%, Aldrich) was used as received. 2,2′-Azobis(4-methoxy-2,4-dimethyl valeronitrile) (V-70, 96%, Wako) was stored at −20 °C and used as received. The alkyl-cobalt(III) adduct initiator ([$Co(acac)_2$-(CH(OAc)-CH_2)$_{\sim 4}R_0$] where R_0 is the primary radical generated by V70) was prepared as described previously,[43] and stored as a CH_2Cl_2 solution at −20 °C under argon. All polymerizations were performed by classical Schlenk techniques under argon.

Characterization

The molar masses (M_n) and molar mass distributions (M_w/M_n) of the *N*VCL-based copolymers were determined by size-exclusion chromatography (SEC) in dimethylformamide (DMF) containing LiBr (0.025 M) relative to poly(methyl methacrylate) (PMMA) standards at 55 °C (flow rate: 1 mL min^{-1}) with a Waters 600 liquid chromatograph equipped with a 410 refractive index detector as well as two PSS GRAM analytical columns (1000 Å, 8 × 300 mm, particle size 10 μm) and one PSS GRAM analytical column (30 Å, 8 × 300 mm, particle size 10 μm). The absolute molar masses of the P*N*VCL-*block*-P(*N*MVA-*stat*-*N*VCL) block copolymer and its P*N*VCL precursor were determined by SEC equipped with a multiangle laser light scattering (MALLS) detector in DMF/LiBr (0.025 M). The Wyatt MALLs detector (120 mW solid-state laser, k ¼ 658 nm, DawnHeleos S/N342-H) measures the excess Rayleigh ratio Rh (related to the scattered intensity) at different angles for each slice of the chromatogram. The specific refractive index increment (d*n*/d*c*) of each (co) polymer was measured by using a Wyatt Optilab refractive index detector (k ¼ 658 nm). Data were processed with the Astra V software (Wyatt Technology). ^{1}H NMR spectra of reaction mixtures were recorded in $CDCl_3$ at 298 K with a 250 MHz Bruker spectrometer and ^{1}H NMR spectra of final polymers with a 500 MHz Bruker spectrometer.

Statistical cobalt-mediated radical copolymerization of *N*VCL and vinyl acetamides. A bent 50 mL flask containing *N*VCL (7.80 g, 56.0 mmol) was connected to a 100 mL Schlenk tube equipped with a magnetic bar. The *N*VCL was melted at 40 °C and degassed by three vacuum–argon cycles. A solution of alkyl-cobalt(III) initiator ([$Co(acac)_2$-(CH(OAc)-CH_2)$_{\sim 4}R_0$]) in CH_2Cl_2 was introduced under argon in the 100 mL Schlenk tube (3.0 mL of a 0.032 M stock solution, 9.6 × 10^{-2} mmol) and evaporated to dryness under reduced pressure at room temperature. The melted *N*VCL at 40 °C was then transferred onto the CMRP initiator before addition of *N*MVA (2.0 mL, 1.92 g, 19.3 mmol) under argon (*N*MVA/*N*VCL molar feed ratio = 26/74, $M_{nth,100\%}$ = 101 000 g mol^{-1}). The

Table 1 Statistical cobalt-mediated radical copolymerization of *N*VCL and vinylacetamides in bulk at 40 °C

	In feed (mol%)						In copolymer[a] (mol%)		
Comonomer	Comonomer	*N*VCL	Time (h)	Conv. tot.[a] (%)	M_n[b] (g mol^{-1})	M_w/M_n[b]	Comonomer	*N*VCL	T_{CP}[c] (°C)
*N*MVA	14	86	3.25	38	25 000	1.05	10	90	43.3
	26	74	3	30	20 300	1.06	19	81	50.6
	38	62	8	36	33 400	1.09	29	71	57.0
	48	52	3	30	35 600	1.17	37	63	66.9
*N*VA	10	90	4.5	35	24 200	1.11	9	91	42.2
	20	80	1.7	37	26 500	1.05	22	78	47.5
	25	75	1.8	31	31 300	1.05	24	76	49.3
	30	70	2.0	41	31 000	1.05	32	68	53.7
	40	60	1.5	37	34 900	1.05	45	55	63.5
	50	50	1.5	38	39 600	1.06	57	43	80.7

[a] Determined by ^{1}H NMR in $CDCl_3$. [b] Determined by SEC in DMF (calibration PMMA). [c] Measured by turbidimetry (at 700 nm) in water (1 g L^{-1}). In all the experiments, the $[comonomers]_0/[R\text{-}Co(acac)_2]_0$ ratio was adjusted to target a molar mass of 1×10^5 g mol^{-1} at full conversion.

reaction mixture was stirred at 40 °C and the monomer conversion was monitored by ^{1}H NMR spectroscopy in $CDCl_3$. After 3 h, the monomer conversion reached 30% and a degassed solution of TEMPO (0.3 mmol) in DMF (4 mL) was injected into the medium in order to stop the polymerization and eliminate the cobalt complex from the copolymer chain-end, according to a previous report.[46] The polymer was recovered by precipitation in diethylether (Et_2O, 250 mL), filtered, dried under reduced pressure and purified by overnight dialysis in deionized water using a Spectra/Por®1 membrane (6–8 kD). The final P(*N*VCL-*stat*-*N*MVA) copolymer was collected as a white powder after lyophilization of the aqueous solution. The molecular parameters of the copolymer were measured by SEC in DMF using PMMA as a calibration ($M_{n,SEC}$ = 20 300 g mol^{-1}, M_w/M_n = 1.06) or a MALLS detector ($M_{n,MALLS}$ = 23 600 g mol^{-1}, dn/dc = 0.0852 mL g^{-1}). The composition of the copolymer was determined by ^{1}H NMR in $CDCl_3$ (*N*MVA/*N*VCL molar ratio in the copolymer = 19/81) (Fig. S1a†).

Similar experiments were carried out with various *N*MVA/*N*VCL molar ratios (Table 1). The exact molar masses of the statistical copolymers were determined by SEC-MALLS in DMF: *N*MVA/*N*VCL molar ratio in the copolymer = 10/90, dn/dc = 0.0847 mL g^{-1}, $M_{n,MALLS}$ = 31 100 g mol^{-1}; *N*MVA/*N*VCL molar ratio in the copolymer = 29/71, dn/dc = 0.0868 mL g^{-1}, $M_{n,MALLS}$ = 37 700 g mol^{-1}.

The same procedure was used for the statistical copolymerization of *N*VCL and *N*VA except that both solid monomers were initially mixed and conditioned together under argon in the bent flask before being melted and transferred onto the CMRP initiator. Data are presented in Table 1.

Statistical cobalt-mediated radical copolymerization of *N*VCL and vinylesters. Various amounts of VAc or VPi were substituted for *N*MVA in the above-mentioned procedure in order to prepare the P(*N*VCL-*stat*-VAc) and P(*N*VCL-*stat*-VPi) copolymers. Detailed reaction conditions and characteristics of the copolymers are shown in Table 2.

Synthesis of the P*N*VCL-*block*-P(*N*MVA-*stat*-*N*VCL) block copolymer. A bent 50 mL flask containing *N*VCL (3.60 g, 25.9 mmol) was connected to a 100 mL Schlenk tube equipped with a magnetic bar. The *N*VCL was melted at 40 °C and degassed by three vacuum–argon cycles. A solution of alkylcobalt(III) initiator ($[Co(acac)_2\text{-}(CH(OAc)\text{-}CH_2)_{\sim 4}R_0]$) in CH_2Cl_2 was introduced under argon in the 100 mL Schlenk tube (0.2 mL of a 0.18 M stock solution, 3.6 10^{-2} mmol) and evaporated to dryness under reduced pressure at room temperature. The melted *N*VCL at 40 °C was then transferred onto the CMRP

Table 2 Statistical cobalt-mediated radical copolymerization of *N*VCL and vinyl esters in bulk at 40 °C

	In feed (mol%)						In copolymer[a] (mol%)		
Comonomer	Comonomer	*N*VCL	Time (h)	Conv. tot.[a] (%)	M_n[b] (g mol)	M_w/M_n[b]	Comonomer	*N*VCL	T_{CP}[c] (°C)
VAc	10	90	2.6	33	26 000	1.05	11	89	35.9
	20	80	2.5	28	36 200	1.05	15	85	35.0
	30	70	7.0	31	39 500	1.05	27	73	30.6
	40	60	48	28	33 300	1.24	31	69	27.1
	50	50	115	26	35 400	1.42	40	60	22.2
	60	40	115	25	45 500	1.36	45	55	19.4
VPi	5	95	1.2	27	24 050	1.06	7	93	32.6
	10	90	2.0	29	22 000	1.05	10	90	29.8
	15	85	2.0	29	23 900	1.06	14	86	27.1
	25	75	4.0	31	29 300	1.07	23	77	20.8

[a] Determined by ^{1}H NMR in $CDCl_3$. [b] Determined by SEC in DMF (calibration PMMA). [c] Measured by turbidimetry (at 700 nm) in water (1 g L^{-1}). In all the experiments, the $[comonomers]_0/[R\text{-}Co(acac)_2]_0$ ratio was adjusted to target a molar mass of 1×10^5 g mol^{-1} at full conversion.

initiator ($M_{nth,100\%}$ = 100 000 g mol^{-1}). The reaction mixture was heated at 40 °C under stirring and ^{1}H NMR analyses of aliquots were carried out to follow the monomer conversion. When the *N*VCL consumption reached 30%, a sample was picked out of the medium, diluted in DMF and added with traces of TEMPO before SEC-MALLS analysis (d*n*/d*c* of P*N*VCL = 0.083 mL g^{-1}, M_n = 43 860 g mol^{-1}, M_w/M_n = 1.033). Then, *N*MVA (2.6 mL, 26.3 mmol) was added under argon to the reaction mixture with the residual *N*VCL and the polymerization was pursued at 40 °C (comonomer feed *N*MVA/*N*VCL: 59/41). After 5.5 h, based on the ^{1}H NMR spectrum of the reaction mixture in $CDCl_3$, 30% of total monomer conversion was achieved and a degassed solution of TEMPO (1.2 mmol) in DMF (4 mL) was injected into the medium in order to stop the polymerization and to remove the cobalt complex from the copolymer chain-end.[46] The copolymer was precipitated in diethylether (250 mL) from a DMF solution, filtered, dried and purified by dialysis using a Spectra/Por®1 membrane (6–8 kD) in deionized water. The P*N*VCL-*block*-P(*N*MVA-*stat*-*N*VCL) copolymer was collected as a white powder after lyophilization of the aqueous solution. SEC-MALLS measurements were carried out in DMF in order to determine the molecular parameters of the copolymer (d*n*/d*c* of P*N*VCL-*block*-P(*N*MVA-*stat*-*N*VCL) = 0.0778 mL g^{-1}, $M_{n,MALLS}$ = 84 980 g mol^{-1}, $M_{n,SEC,cal,PMMA}$ = 64 300 g mol^{-1}, M_w/M_n = 1.13). The composition of P(*N*MVA-*stat*-*N*VCL) block was given by ^{1}H NMR (60/40: *N*MVA/*N*VCL).

Aqueous solution behavior. The transmittance of the aqueous solutions of polymers (1 g L^{-1} and 5 g L^{-1}) was recorded on a Jasco V630 UV-vis spectrophotometer at 700 nm equipped with a temperature controller system (ETCS-761). The heating/cooling rate was 1 °C min^{-1} between 10 °C and 80 °C. The cloud point temperature (T_{CP}) was defined at the half drop transmittance from the initial transmittance. DLS experiments were performed on a Malvern CGS-3 apparatus equipped with a He–Ne laser with a wavelength of 633 nm. The measurements were performed in water at 90° angle at a concentration of 1 g L^{-1}. Data were analyzed using the CONTIN method which is based on an inverse-Laplace transformation of the data and gives access to a size distribution histogram.

TEM was carried out with a Philips CM 100 operating at a voltage of 100 kV, equipped with a Megaview G2 camera. A droplet of the P*N*VCL-*b*-P(*N*VCL-*co*-*N*MVA) aqueous solution (1 g L^{-1}) thermostatted at 60 °C was spin coated on a Formvar-coated copper grid.

The variable temperature ^{1}H NMR measurements on the P*N*VCL-*block*-P(*N*MVA-*stat*-*N*VCL) copolymer were carried out in D_2O (4 g L^{-1}) on a Bruker Avance spectrometer operating at 500 MHz at different temperatures ranging from 22 °C to 60 °C.

Results and discussion

Controlled synthesis of *N*VCL-based statistical copolymers with tunable LCST

The controlled radical copolymerization of *N*VCL with hydrophilic *N*-vinylamides or hydrophobic vinyl esters was investigated by CMRP (Scheme 2) using $Co(acac)_2$ as a controlling agent

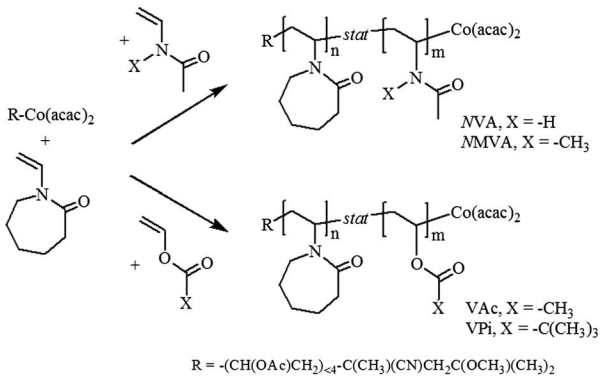

Scheme 2 Statistical cobalt-mediated radical copolymerization of *N*-vinylcaprolactam with *N*-vinylamides or vinylesters.

because its ability to mediate the polymerization of such non-conjugated monomers has been clearly demonstrated.[39] The copolymerization experiments were performed in bulk at 40 °C using a low molecular weight alkyl-cobalt(III) adduct initiator (R-Co(acac)$_2$) synthesized and characterized elsewhere.[43]

*N*VCL was first copolymerized by CMRP with various amounts of *N*MVA or *N*VA. The tested comonomers feed ratios are listed in Table 1. For all these experiments, the targeted molar mass of the copolymers P(*N*VCL-*stat*-*N*MVA) and P(*N*VCL-*stat*-*N*VA) at full monomer conversion was equal to 1 × 10^5 g mol^{-1} and polymerizations were stopped at around 30–40% conversion in order to ensure a very good control of the copolymerization. Copolymers with low molar mass distribution ($M_w/M_n \sim$ 1.1) and molar mass around 30 000 g mol^{-1} were collected as determined by SEC. The composition of the final copolymers was determined by ^{1}H NMR (see ESI, Fig. S1†). It is also worth noting that the *N*VCL/*N*VA copolymerization is properly controlled although we know that the homopolymerization of *N*VA carried out under the same conditions results in a high molar mass P*N*VA with broad molar mass distribution.[34] As expected based on the previously reported reactivity ratios (r_{NVCL} = 0.46, r_{NMVA} = 0.28),[31] the content of *N*MVA is a little bit lower in the copolymer than in the monomer feed. In contrast, we found that *N*VA incorporates slightly better than *N*VCL in the copolymer. Below, we discuss the influence of the composition of these poly(*N*-vinylamide) copolymers on their LCST.

$Co(acac)_2$ is also known as an excellent controlling agent for the polymerization of vinyl esters, which was a strong incentive to copolymerize *N*VCL with the more hydrophobic VAc and VPi in order to adjust downward the phase transition temperature of the *N*VCL containing copolymer. The copolymerizations were also performed in bulk at 40 °C (Table 2). As expected, well-defined P(*N*VCL-*stat*-VAc) and P(*N*VCL-*stat*-VPi) copolymers ($M_w/M_n \sim$ 1.1) with various compositions were prepared accordingly. We noticed that the *N*VCL/VAc statistical copolymerization rate was significantly low and a moderate increase of the molar mass distribution was observed ($M_w/M_n \sim$ 1.3–1.4) when the VAc content exceeds 40% in the feed. Moreover, the ^{1}H NMR analyses revealed that the incorporation of *N*VCL in the copolymer is slightly easier than that of VAc, in agreement with the reported reactivity ratios (r_{NVCL} = 1.06, r_{VAc} = 0.36).[31] In

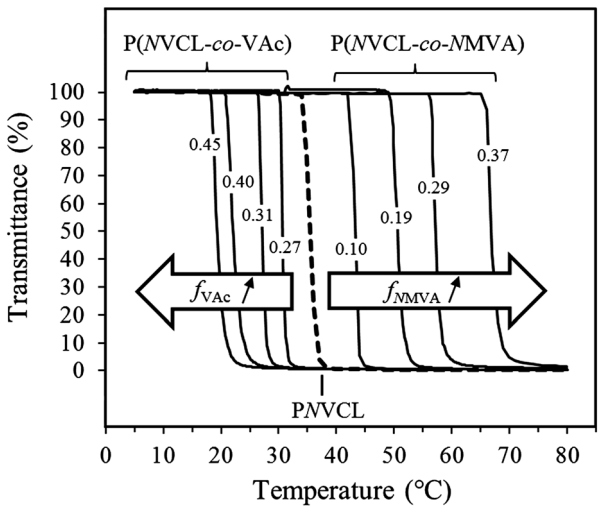

Fig. 1 Turbidimetry analysis of aqueous solutions of P(*N*VCL-*stat*-*N*MVA) and P(*N*VCL-*stat*-VAc) copolymers with various compositions (temperature ramp = 1 °C min^{-1}). The T_{CP} values of the copolymer solutions are reported in Tables 1 and 2.

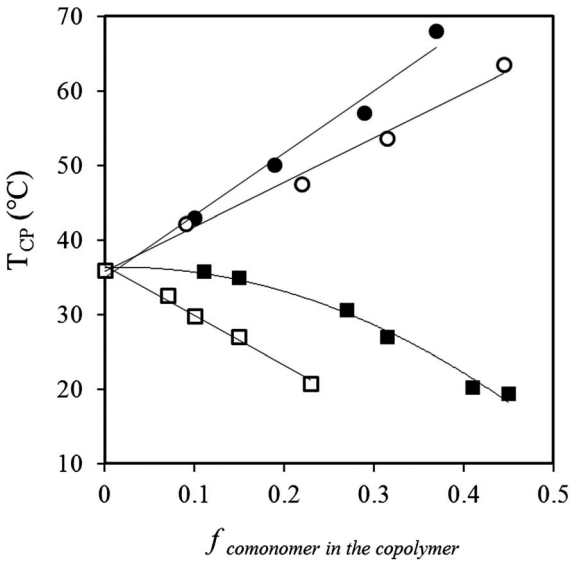

Fig. 2 Evolution of the cloud point temperature (T_{CP}) of the *N*VCL-based copolymer aqueous solutions with the comonomer molar fraction in the copolymer (*f*). *N*MVA (●), *N*VA (○), VAc (■), and VPi (□).

contrast, in the *N*VCL/VPi copolymerization, the compositions of the feeds and the copolymers were similar.

Next, we studied the effect of the nature and the content of comonomers on the LCST of these copolymers. The cloud point temperature of the aqueous solution of each copolymer (0.1 wt %) was measured by turbidimetry. Fig. 1 shows the transmittance *versus* temperature plots, also called cloud point curves, for various P(*N*VCL-*stat*-*N*MVA) and P(*N*VCL-*stat*-VAc) copolymer solutions. A heating rate of 1 °C min^{-1} was used and we considered that the cloud point was reached when half of the transmittance of the solution was lost. For the sake of comparison, an aqueous solution of pure P*N*VCL, prepared by CMRP (M_n = 54 000 g mol^{-1}, M_w/M_n = 1.21), was analyzed as described above (dotted line in Fig. 1); a T_{CP} of 36 °C was found. Considering Fig. 1, the cloud point curves are substantially shifted towards higher temperatures upon incorporation of increasing amounts of hydrophilic *N*MVA in the copolymer. For example, T_{CP} reached 67 °C when the molar fraction of *N*MVA in the copolymer (f_{NMVA}) was equal to 0.37. In contrast, the copolymerization of *N*VCL with increasing amounts of VAc, which is more hydrophobic than *N*VCL, decreased the T_{CP} of the copolymer solution. The latter could be reduced to 19 °C when the VAc content in the copolymer reached 45%.

The transmittance of the P(*N*VCL-*stat*-*N*VA) and P(*N*VCL-*stat*-VPi) aqueous solutions was also monitored between 10 °C and 80 °C. The recorded phase transition temperatures are listed in Tables 1 and 2 and charted as a function of the comonomer molar fraction in the copolymer ($f_{comonomer}$) (Fig. 2). For both hydrophilic vinyl acetamides, we observed a positive and linear evolution of the T_{CP} with the comonomer content in the *N*VCL-based copolymers, and this increase was slightly lower for *N*VA compared to *N*MVA. On the other hand, a more pronounced decrease of the T_{CP} of the copolymer was found when VAc was replaced by a more hydrophobic comonomer, *i.e.* VPi. Indeed, the incorporation of 25 mol% of VPi in the copolymer was enough to reduce the T_{CP} to 20 °C whereas 45 mol% of VAc was necessary to observe the same effect.

Finally, the reversibility of the temperature induced phase transition was investigated for all the copolymers and we found that hysteresis never exceeds a few degrees (see ESI, Table S1†).

Design of double thermoresponsive *N*VCL-based block copolymers

A great advantage of the CRP methods, and CMRP in particular, over free radical polymerization is the possible synthesis of well-defined block copolymers by sequential polymerization of comonomers. In line with the above-mentioned study on the statistical cobalt-mediated radical copolymerization of *N*-vinylamides, we built for the first time a poly(*N*-vinylamide) containing a block copolymer with two discrete LCSTs. The targeted P*N*VCL-*block*-P(*N*MVA-*stat*-*N*VCL) copolymer was easily obtained by the sequential CMRP of *N*VCL followed by the statistical copolymerization of *N*VCL and *N*MVA (*N*MVA/*N*VCL: 60/40) (Scheme 3). First, the bulk polymerization of *N*VCL was performed at 40 °C using a [*N*VCL]/[R-Co(acac)$_2$] molar ratio equal to 720. When the *N*VCL conversion reached 30%, an appropriate amount of *N*MVA was added to the medium under an inert atmosphere in order to adjust the composition of the monomer feed to 60/40 (*N*MVA/*N*VCL molar ratio). The copolymerization was stopped when the total monomer conversion reached 30% by addition of TEMPO. As reported elsewhere, such a treatment with TEMPO is an efficient method for removing the cobalt complex from polymers prepared by CMRP.[46] According to the overlay of the SEC chromatograms of the polymers before and after addition of *N*MVA (Fig. S2†), the chain extension from the P*N*VCL-Co(acac)$_2$ segment was successful and a block copolymer with low molar mass distribution (M_w/M_n = 1.13) was formed. A low amount of residual homoP*N*VCL (~7%) was detected on the SEC chromatograms but it should not interfere with the self-assembly of the copolymer except slightly increasing the volume of the P*N*VCL phase of

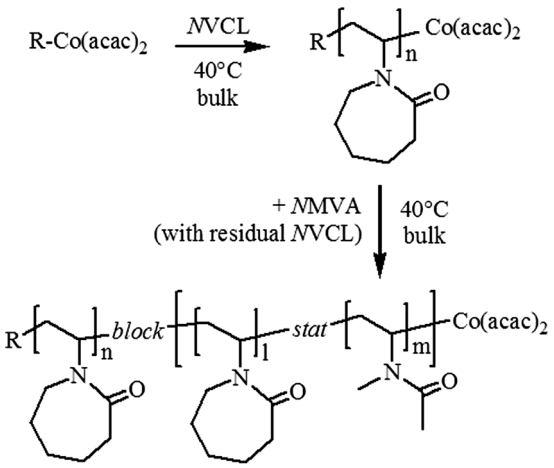

Scheme 3 One-pot strategy for the synthesis of double thermoresponsive P*N*VCL-*block*-P(*N*MVA-*stat*-*N*VCL) block copolymers.

the assemblies. The exact molar masses and the composition of both blocks were determined by combination of SEC analyses using a multiangle laser light scattering (MALLS) detector and ^{1}H NMR measurements ($M_{n,PNVCL,block}$ = 43 860 g mol^{-1}, $M_{n,P(NMVA\text{-}stat\text{-}NVCL),block}$ = 41 120 g mol^{-1}, *N*MVA/*N*VCL units in the second block = 60/40, P*N*VCL$_{315}$-*block*-P(*N*MVA$_{215}$-*stat*-*N*VCL$_{143}$)).

Two distinct thermal transitions were expected upon heating this P*N*VCL-*block*-P(*N*MVA-*stat*-*N*VCL) in water; the LCST of the statistical P(*N*MVA-*stat*-*N*VCL) block should be higher than the one of the homo-P*N*VCL sequence. In theory, the copolymer should exhibit gradual transitions from hydrophilic to amphiphilic, and finally to hydrophobic, when the sample is heated (Fig. 3). Both blocks should be soluble in water at low temperature, only P*N*VCL should dehydrate at a temperature between the two LCSTs, and the P(*N*MVA-*stat*-*N*VCL) block should also become hydrophobic at higher temperature. A visual inspection of the copolymer solution at different temperatures was quite instructive (see pictures in Fig. 3). It remained clear below 40 °C as expected for fully hydrated chains, opalescent between 40 °C and 70 °C suggesting the assembly of the copolymer into micelles, and opaque above 70 °C due to the collapse of the polymer chains. Repeated heating–cooling cycles indicated that these thermal transitions are reversible. The thermal behavior of this double thermoresponsive block copolymer in water was further investigated and discussed hereafter.

The thermally induced phase separation and self-assembly behavior of the P*N*VCL-*block*-P(*N*MVA-*stat*-*N*VCL) copolymer in water (1 g L^{-1}) were first evaluated by turbidimetry at a heating rate of 1 °C per minute (Fig. 4a) and DLS (Fig. 4b and c). Four distinct regions appeared from 25 °C to 80 °C.

Below 37 °C (region I), the transmittance of the solution remained maximum (Fig. 4a) and the scattered intensity was very low (Fig. 4b), indicating that both blocks of the copolymer were fully solvated. In agreement with this observation, DLS

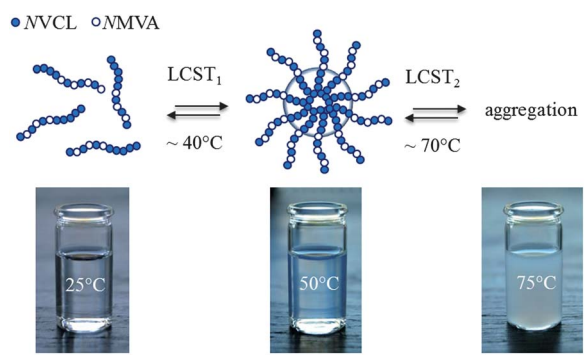

Fig. 3 General scheme for the thermally induced phase transitions of the P*N*VCL-*block*-P(*N*MVA-*stat*-*N*VCL) aqueous solution. Pictures of the copolymer solution (1 g L^{-1}) were taken at temperatures representative of each regime (free chains–micelles–aggregates).

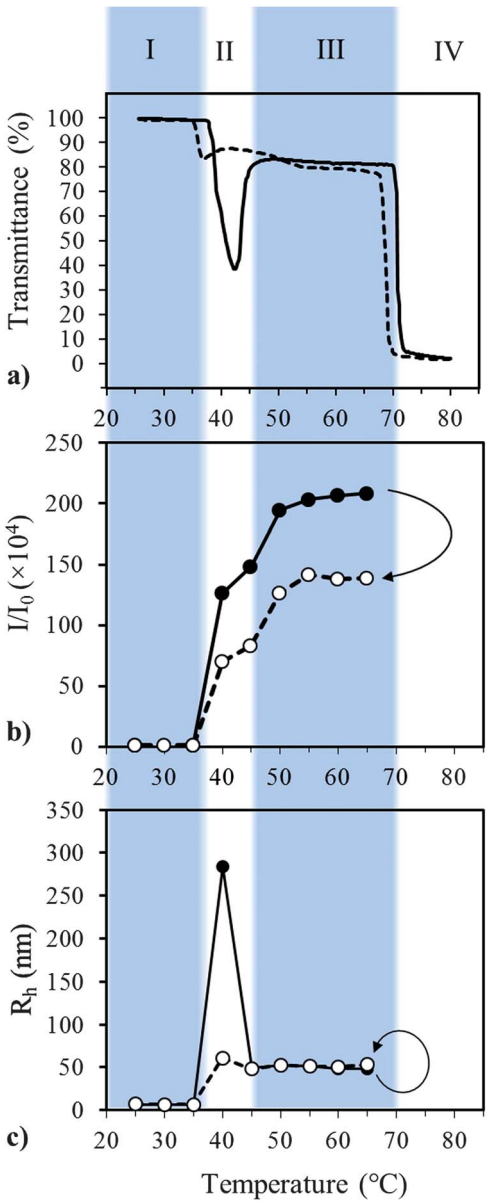

Fig. 4 Transmittance (1 °C min^{-1}) (a), scattered intensity measured by DLS (b) and apparent hydrodynamic radius measured by DLS (c) of the P*N*VCL-*b*-P(*N*MVA-*stat*-*N*VCl) aqueous solution (1 g L^{-1}) as a function of temperature. Full line and dotted line correspond to the heating and cooling process, respectively.

results showed a large number of objects with an apparent hydrodynamic radius (R_h) of 7 nm (Fig. 4c), which correspond to unimers (free solvated chains). A limited number of aggregates ($R_h \sim 100$ nm) were also detected and are visible on the full size distribution (Fig. S3,† at 30 °C).

Above 37 °C, the solution became turbid and the transmittance dropped down, with a minimum of 40% at 42 °C (Fig. 4a, region II). This sudden increase of the solution turbidity is due to the dehydration of the P*N*VCL block (see below). In parallel, an increase in the scattered intensity was observed (Fig. 4b) and large size aggregates were detected (R_h = 284 nm at 40 °C, Fig. 4c) (see Fig. S3† for the full size distribution). The size of these objects remained constant when the solution was kept at 40 °C for at least one hour. However, a further heating of the system caused the reorganization of the copolymer as assessed by the recovery in the transmittance (80% at 45 °C) and the transformation of the large aggregates into small particles (R_h = 50 nm). These particles are micelles made of a fully dehydrated P*N*VCL core stabilized by a solvated P(*N*MVA-*stat*-*N*VCL) shell. Similar evolutions of the turbidity and the particle size have been previously reported and commented for other thermoresponsive block copolymers.[18–20] It was suggested that the dehydration of the thermosensitive block at the onset of the phase separation is sufficient to induce the clouding of the solution but not sufficient to induce the proper micellization of the copolymer, the latter requiring a further (small) increase of the temperature. In this respect, the increase of the scattered intensity, together with the decrease in size, observed in DLS between 40 °C and 45 °C (Fig. 4b) is explained by the transformation of the initial loose (swollen) aggregates into smaller particles with a dense core, *i.e.* micelles.

These micelles, resulting from the selective dehydration of the P*N*VCL block of the copolymer, were stable between 45 °C and 70 °C (region III). In this interval, the transmittance is constant, the scattered intensity curve reached a plateau, and the radius of the particles ($R_h \sim 50$ nm) does not change (Fig. 4c and full size distribution in Fig. S3†). A drop of the copolymer solution thermostatted at 60 °C was spin-coated on a TEM copper grid in order to visualize the micelles (Fig. S4†). The particles observed by TEM were spherical and their size (diam. = 20–50 nm) appeared smaller compared with the DLS data. This is a very common observation explained by the fact that the sample studied by TEM is in the dry state, which can cause the contraction of the objects, and moreover often only the core of the particles is dense enough to be observed by electronic microscopy.

At 70 °C, a last transition occurred, as indicated by the complete loss of transmittance beyond this temperature (region IV, Fig. 4a). The latter corresponds to the dehydration of the P(*N*MVA-*stat*-*N*VCL) shell of the particles leading to the total collapse of the copolymer. The DLS analysis of the copolymer solution at 70 °C is provided in Fig. S3† and confirms the presence of aggregates. It is also clear that the LCST of the second block, composed of 60 mol% of *N*MVA, is affected and lowered by the P*N*VCL block. Indeed, according to our previous study (Fig. 2), a T_{CP} equal to 70 °C is rather typical of P(*N*MVA-*stat*-*N*VCL) copolymers composed of 40 mol% of *N*VMA.

The reversibility of the temperature induced transitions was also demonstrated by cooling the white turbid solution from 80 °C to 25 °C at a rate of 1 °C per minute (see the dotted line in Fig. 4a). Aggregated polymer chains, micelles and free copolymer chains were successfully observed in water upon cooling (see the dotted line in Fig. 4c). In addition, the transition temperature differed only by two degrees in comparison with the heating process. It is worth noting that the disruption of the polymer micelles did not transit by large and loose aggregates (see dotted lines in Fig. 4a and c) as during the heating. Four consecutive heating–cooling cycles of the block copolymer were monitored by turbidimetry and the almost perfect overlay of the transmittance profiles confirms the repeatability of the thermal response (Fig. S5a†). DLS measurements performed during the second cycle also showed aggregates (R_h = 210 nm) at 40 °C and smaller particles at 55 °C (R_h = 55 nm) (Fig. S5b†).

The P*N*VCL-*block*-P(*N*MVA-*stat*-*N*VCL) was also analyzed at various temperatures by ^{1}H NMR spectroscopy at a concentration of 4 g L^{-1} in D_2O (Fig. 5). NMR is a powerful technique for the characterization of thermoresponsive block copolymers because only hydrated polymer segments are detected and the transition temperature can be easily identified. First, we checked that the turbidimetry curve at 4 g L^{-1} was similar to the one at 1 g L^{-1}. A series of ^{1}H NMR spectra were then recorded between 22 °C and 59 °C (Fig. 5). The characteristic signals of both *N*VCL (denoted a–e, Fig. 5) and *N*MVA (denoted 1–4, Fig. 5) units in the copolymer did not change upon heating the solution from 22 °C to 30 °C, which confirms that the P*N*VCL-*block*-P(*N*MVA-*stat*-*N*VCL) copolymer is soluble in D_2O. However, signals of the *N*VCL, *e.g.* methylene protons b at 3.3 ppm and c at 2.4 ppm, sharply decreased from 35 °C to 41 °C. In contrast, the intensity of the signals corresponding to the *N*MVA units, *e.g.* methyl protons 2 at 2.8 ppm, remained constant in this temperature range. The onset of the dehydration of the P*N*VCL block measured by NMR is in agreement with the turbidimetry data. At 41 °C, the dehydration of the P*N*VCL block is high but not complete. Indeed, signals of P*N*VCL keep on decreasing until 45 °C. In conjunction with the DLS data, this experiment

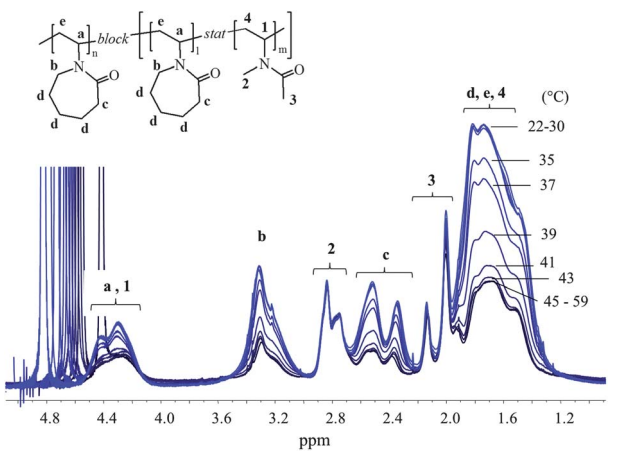

Fig. 5 ^{1}H NMR spectra evolution of the P*N*VCL-*block*-P(*N*MVA-*stat*-*N*VCL) copolymer in D_2O (4 g L^{-1}) upon elevating the solution temperature from 22 °C to 59 °C.

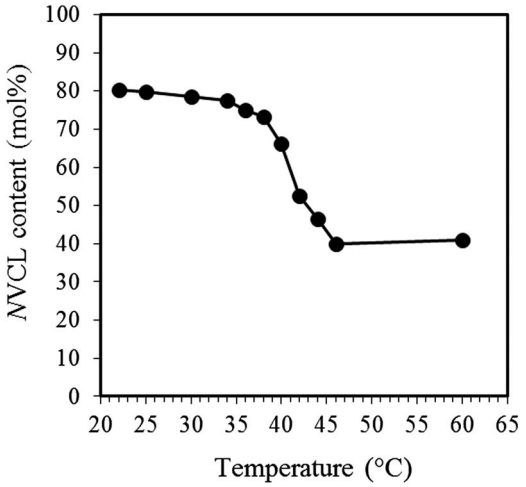

Fig. 6 Temperature dependence of the *N*VCL content in the hydrated parts of the P*N*VCL-*block*-P(*N*MVA-*stat*-*N*VCL) followed by ^{1}H NMR analysis in D_2O at a polymer concentration of 4 g L^{-1}.

confirms that the loose aggregates observed at 41 °C require a further dehydration of the P*N*VCL chains, achieved at 45 °C, in order to transform themselves into smaller micelles. The NMR spectra of the copolymer solution at 45 °C and 59 °C were identical and correspond to the P(*N*VCL-*co*-*N*MVA) solvated shell of the micelles in D_2O.

Based on the relative intensities of the *N*VCL and *N*MVA signals in the copolymer ^{1}H spectra, we charted the evolution of the *N*VCL content in the hydrated parts of the P*N*VCL-*block*-P(*N*MVA-*stat*-*N*VCL) copolymer as a function of temperature (Fig. 6). In good agreement with turbidimetry and DLS data, the dehydration of the P*N*VCL starts at around 35 °C and goes on until 45 °C. Between 45 °C and 60 °C, the copolymer forms micelles where only the P(*N*MVA-*stat*-*N*VCL) block, forming the shell of the micelles, is solvated. This is indeed reflected in Fig. 6 which shows a *N*VCL content around 40 mol% in this temperature range, in good agreement with the comonomer feed (*N*VCL/*N*MVA: 40/60) used for the synthesis of the second block of the P*N*VCL-*block*-P(*N*MVA-*stat*-*N*VCL) copolymer.

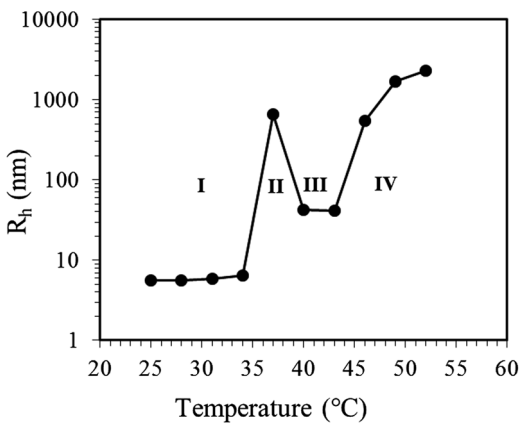

Fig. 7 Evolution of the apparent hydrodynamic radius measured by DLS as a function of temperature for the P*N*VCL$_{252}$-*block*-P(*N*MVA$_{85}$-*stat*-*N*VCL$_{127}$) ($M_{n,MALLS}$ = 56 000 g mol^{-1}, M_w/M_n = 1.13, d*n*/dc = 0.0875 mL g^{-1}) copolymer in water (1 g L^{-1}).

A second double thermoresponsive P*N*VCL-*block*-P(*N*MVA-*stat*-*N*VCL) copolymer was prepared following the same strategy in order to demonstrate that the transition temperatures can be tuned by changing the composition of the blocks. As a confirmation, when the P*N*VCL segment (35 000 g mol^{-1}) is associated with a P(*N*MVA-*stat*-*N*VCL) block (21 000 g mol^{-1}) containing only 40 mol% of *N*MVA, the same regimes (I to IV) were observed by DLS (Fig. 7) and turbidimetry (Fig. S6†) except that both cloud point temperatures were closer to each other. Nevertheless, well-defined particles (R_h = 42 nm, PDI = 0.12) were formed around 40 °C (see region III in Fig. 7), which confirms that the "micellar window" can be adjusted by tuning the composition of the blocks.

Conclusions

The statistical radical copolymerization of *N*VCL with hydrophilic *N*-vinylamides (*N*VA, *N*MVA) and hydrophobic vinylesters (VAc, VPi) was performed for the first time in a controlled fashion. A range of well-defined *N*VCL-containing statistical copolymers with different compositions were produced by CMRP using $Co(acac)_2$ as a mediator. The LCST of each copolymer was measured in water by turbidimetry in order to establish the temperature dependence of the phase transition with the comonomer nature and content. As a result, the LCST of the *N*VCL-based copolymers can now be precisely tuned up and down by incorporating increasing amounts of *N*-vinylacetamides and vinylesters, respectively. This study also reports the synthesis of dual thermoresponsive *N*VCL-based block copolymers. The latter were easily obtained by sequential CMRP of *N*VCL followed by the statistical copolymerization of *N*VCL and *N*MVA (*N*MVA/*N*VCL). The thermal behavior of these P*N*VCL-*b*-P(*N*MVA-*stat*-*N*VCL) copolymers was assessed by turbidimetry, TEM, DLS and NMR. Two discrete thermal transitions were detected and were shown to be dependent on the composition of the blocks. Upon increasing the temperature, four different regimes and polymer organizations were observed: free chains below the first LCST, large and loose aggregates around the first transition, compact and small micelles composed of a dehydrated P*N*VCL core and a solvated P(*N*MVA-*stat*-*N*VCL) shell between the two LCSTs, and precipitated copolymer chains above the second LCST. Interestingly, the micelles were stable in size in a quite large temperature range (up to 25 °C) and could also be formed upon cooling the copolymer precipitated in hot water. These advances represent a significant step towards the development of a platform based on thermoresponsive P*N*VCL copolymers with a single phase separation or multistep assembly behaviors.

Acknowledgements

The authors are grateful to the Fonds National de la Recherche Scientifique (FRS-FNRS) and to the Belgian Science Policy for financial support in the frame of the Interuniversity Attraction Poles Programme (P7/05)–Functional Supramolecular Systems

(FS2) for the financial support. A. D. and A. K. are grateful for funding from the University of Liège *via* the "Fonds spéciaux pour la recherche – crédits de démarrage". A. D. and C.-A. F. are research associates of the FRS-FNRS. C. D. is the research director of the FRS-FNRS. The authors also thank G. Cartigny, A. Matagne, J. Herman and C. Le Duff for skillful assistance in MALLS, turbidimetry and NMR measurements, respectively.

Notes and references

1 A. E. Smith, X. Xu and C. L. McCormick, *Prog. Polym. Sci.*, 2010, **35**, 45–93.
2 F. Liu and M. W. Urban, *Prog. Polym. Sci.*, 2010, **35**, 3–23.
3 D. Roy, J. N. Cambre and B. S. Sumerlin, *Prog. Polym. Sci.*, 2010, **35**, 278–301.
4 C. d. l. H. Alarcon, S. Pennadam and C. Alexander, *Chem. Soc. Rev.*, 2005, **34**, 276–285.
5 C. Alexander and K. M. Shakesheff, *Adv. Mater.*, 2006, **18**, 3321–3328.
6 J. Seuring and S. Agarwal, *Macromol. Rapid Commun.*, 2012, **33**(22), 1898–1920.
7 S. Dai, P. Ravi and K. C. Tam, *Soft Matter*, 2009, **5**, 2513–2533.
8 Y. Xia, X. Yin, N. A. D. Burke and H. D. H. Stöver, *Macromolecules*, 2005, **38**, 5937–5943.
9 P. Kujawa, F. Segui, S. Shaban, C. Diab, Y. Okada, F. Tanaka and F. M. Winnik, *Macromolecules*, 2006, **39**, 341–348.
10 S. Aoshima and S. Kanaoka, *Adv. Polym. Sci.*, 2008, **210**, 169–208.
11 S.-I. Yusa, S. Yamago, M. Sugahara, S. Morikawa, T. Yamamoto and Y. Morishima, *Macromolecules*, 2007, **40**, 5907–5915.
12 R. Hoogenboom, *Angew. Chem., Int. Ed.*, 2009, **48**, 7978–7994.
13 C. Weber, R. Hoogenboom and U. S. Schubert, *Prog. Polym. Sci.*, 2012, **37**, 686–714.
14 J.-F. Lutz, *Adv. Mater.*, 2011, **23**, 2237–2243.
15 J.-F. Lutz, *J. Polym. Sci., Part A: Polym. Chem.*, 2008, **46**, 3459–3470.
16 J.-F. Lutz, O. Akdemir and A. Hoth, *J. Am. Chem. Soc.*, 2006, **128**, 13046–13047.
17 I. Dimitrov, B. Trzebicka, A. H. E. Müller, A. Dworak and C. B. Tsvetanov, *Prog. Polym. Sci.*, 2007, **32**, 1275–1343.
18 L. T. T. Trinh, H. M. L. Lambermont-Thijs, U. S. Schubert, R. Hoogenboom and A.-L. Kjoeniksen, *Macromolecules*, 2012, **45**, 4337–4345.
19 K. Skrabania, J. Kristen, A. Laschewsky, O. Akdemir, A. Hoth and J.-F. Lutz, *Langmuir*, 2007, **23**, 84–93.
20 H. Mori, I. Kato, S. Saito and T. Endo, *Macromolecules*, 2010, **43**, 1289–1298.
21 R. Hoogenboom, F. Wiesbrock, M. A. M. Leenen, H. M. L. Thijs, H. Huang, C.-A. Fustin, P. Guillet, J.-F. Gohy and U. S. Schubert, *Macromolecules*, 2007, **40**, 2837–2843.
22 N. Jin, H. Zhang, S. Jin, M. D. Dadmun and B. Zhao, *J. Phys. Chem. B*, 2012, **116**, 3125–3137.
23 P. J. Roth, T. P. Davis and A. B. Lowe, *Macromolecules*, 2012, **45**, 3221–3230.
24 Y. Kotsuchibashi, M. Ebara, K. Yamamoto and T. Aoyagi, *J. Polym. Sci., Part A: Polym. Chem.*, 2010, **48**, 4393–4399.
25 Y. Kotsuchibashi, K. Yamamoto and T. Aoyagi, *J. Colloid Interface Sci.*, 2009, **336**, 67–72.
26 R. K. Madhusudana, B. Mallikarjuna, R. K. S. V. Krishna, S. Siraj, R. K. Chowdoji and M. C. S. Subha, *Colloids Surf., B*, 2012, **102**, 891–897.
27 A. Imaz and J. Forcada, *J. Polym. Sci., Part A: Polym. Chem.*, 2010, **48**, 1173–1181.
28 H. Vihola, A. Laukkanen, L. Valtola, H. Tenhu and J. Hirvonen, *Biomaterials*, 2005, **26**, 3055–3064.
29 F. Meeussen, E. Nies, H. Berghmans, S. Verbrugghe, E. Goethals and F. Du Prez, *Polymer*, 2000, **41**, 8597–8602.
30 O. A. Kuznetsova, Y. E. Kirsh, I. I. Pashkin, I. F. Kuz'kina and V. P. Zubov, *Vysokomol. Soedin., Ser. A*, 2000, **42**, 207–212.
31 I. I. Pashkin, Y. E. Kirsh, V. P. Zubov, T. V. Anisimova, I. F. Kuz'kina, Y. P. Voloshina and A. V. Krylov, *Vysokomol. Soedin., Ser. A*, 1993, **35**, 481–484.
32 M. Beija, J.-D. Marty and M. Destarac, *Chem. Commun.*, 2011, **47**, 2826–2828.
33 D. Wan, Q. Zhou, H. Pu and G. Yang, *J. Polym. Sci., Part A: Polym. Chem.*, 2008, **46**, 3756–3765.
34 A. Debuigne, A. N. Morin, A. Kermagoret, Y. Piette, C. Detrembleur, C. Jérôme and R. Poli, *Chem.–Eur. J.*, 2012, **18**, 12834–12844.
35 M. Hurtgen, J. Liu, A. Debuigne, C. Jérôme and C. Detrembleur, *J. Polym. Sci., Part A: Polym. Chem.*, 2012, **50**, 400–408.
36 M. Hurtgen, C. Detrembleur, C. Jérôme and A. Debuigne, *Polym. Rev.*, 2011, **51**, 188–213.
37 R. Poli, *Angew. Chem., Int. Ed.*, 2006, **45**, 5058–5070.
38 L. E. N. Allan, M. R. Perry and M. P. Shaver, *Prog. Polym. Sci.*, 2012, **37**, 127–156.
39 A. Debuigne, R. Poli, C. Jérôme, R. Jérôme and C. Detrembleur, *Prog. Polym. Sci.*, 2009, **34**, 211–239.
40 A. Debuigne, J.-R. Caille and R. Jérôme, *Angew. Chem., Int. Ed.*, 2005, **44**, 1101–1104.
41 A. Debuigne, N. Willet, R. Jérôme and C. Detrembleur, *Macromolecules*, 2007, **40**, 7111–7118.
42 A. Debuigne, M. Schoumacher, R. Riva, N. Willet, X. Zhu, S. Ruetten, C. Jérôme and C. Detrembleur, *Chem. Commun.*, 2011, **47**, 12703–12705.
43 A. Debuigne, Y. Champouret, R. Jérôme, R. Poli and C. Detrembleur, *Chem.–Eur. J.*, 2008, **14**, 4046–4059.
44 D. N. Bunck, G. P. Sorenson and M. K. Mahanthappa, *J. Polym. Sci., Part A: Polym. Chem.*, 2011, **49**, 242–249.
45 R.-P. Nze, O. Colombani and E. Nicol, *J. Polym. Sci., Part A: Polym. Chem.*, 2012, **50**, 4046–4054.
46 A. Debuigne, J.-R. Caille and R. Jérôme, *Macromolecules*, 2005, **38**, 5452–5458.